Science of the Total Environment 662 (2019) 672–686

Contents lists available at ScienceDirect

Science of the Total Environment

journal homepage: www.elsevier.com/locate/scitotenv

Future drought risk in Africa: Integrating vulnerability, climate change, and population growth

Ali Ahmadalipour [a,*], Hamid Moradkhani [a], Andrea Castelletti [b], Nicholas Magliocca [c]

[a] Center for Complex Hydrosystems Research, Department of Civil, Construction, and Environmental Engineering, University of Alabama, Tuscaloosa, AL, United States
[b] Department of Electronics, Information, and Bioengineering, Politecnico di Milano, Milan, Italy
[c] Department of Geography, University of Alabama, Tuscaloosa, AL, United States

HIGHLIGHTS

- Drought risk is studied in Africa by integrating hazard, vulnerability and exposure.
- Multi-model and multi-scenarios are employed at a national level.
- Uncertainty of each risk component is characterized for each country.
- The role of climate change, population growth and vulnerability on risk is explored.
- The spatiotemporal patterns of drought risk and its uncertainties are identified.

GRAPHICAL ABSTRACT

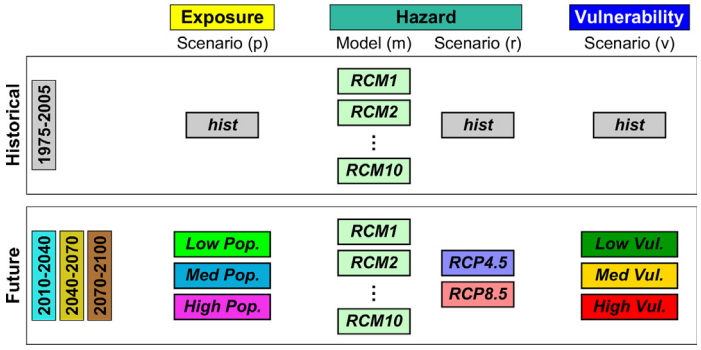

ARTICLE INFO

Article history:
Received 6 November 2018
Received in revised form 27 December 2018
Accepted 21 January 2019
Available online 23 January 2019

Editor: José Virgílio Cruz

Keywords:
Africa
Drought
Risk
Climate change
Vulnerability
Population growth

ABSTRACT

Drought risk refers to the potential losses from hazard imposed by a drought event, and it is generally characterized as a function of vulnerability, hazard, and exposure. In this study, drought risk is assessed at a national level across Africa, and the impacts of climate change, population growth, and socioeconomic vulnerabilities on drought risk are investigated. A rigorous framework is implemented to quantify drought vulnerability considering various sectors including economy, energy and infrastructure, health, land use, society, and water resources. Multi-model and multi-scenario analyses are employed to quantify drought hazard using an ensemble of 10 regional climate models and a multi-scalar drought index. Drought risk is then assessed in each country for 2 climate emission pathways (RCP4.5 and RCP8.5), 3 population scenarios, and 3 vulnerability scenarios during three future periods between 2010 and 2100. Drought risk ratio is quantified, and the role of each component (i.e. hazard, vulnerability, and exposure) is identified, and the associated uncertainties are also characterized. Results show that drought risk is expected to increase in future across Africa with varied rates for different models and scenarios. Although northern African countries indicate aggravating drought hazard, drought risk ratio is found to be highest in central African countries as a consequent of vulnerability and population rise in that region. Results indicate that if no climate change adaptation is implemented, unprecedented drought hazard and risk will occur decades earlier. In addition, controlling population growth is found to be imperative for mitigating drought risk in Africa (even more effective than climate change mitigation), as it improves socioeconomic vulnerability and reduces potential exposure to drought.

* Corresponding author.
E-mail addresses: aahmada@ua.edu (A. Ahmadalipour), hmoradkhani@ua.edu (H. Moradkhani).

https://doi.org/10.1016/j.scitotenv.2019.01.278
0048-9697/

1. Introduction

Drought is one of the most disruptive natural hazards which affects millions of people worldwide each year and imposes substantial challenges to the environment, economy, and society (Carrao et al., 2016; Mishra et al., 2017). It is considered the most damaging natural disaster due to its prolonged and extensive socioeconomic impacts (Carrão et al., 2017; Gudmundsson and Seneviratne, 2016; Mukherjee et al., 2018). Such impacts can either be direct (e.g. restrictions on water use or decreasing crop yield) or indirect (e.g. increasing food costs due to decreased crop yield) (Blauhut et al., 2015a; Stagge et al., 2015).

Droughts impose an average of $6–8 billion damage to the United States each year (Smith and Katz, 2013; Smith and Matthews, 2015). It has been reported that drought damages in Europe during the past three decades has exceeded €100 billion (Carrao et al., 2016). While the wealthy industrialized nations are considerably affected by the economic impacts of drought, its social impacts are remarkable in the food-scarce developing countries with high dependency on agriculture (Below et al., 2007; Schilling et al., 2012). The Ethiopia/Sudan drought of 1974 and the Sahel drought of 2007 were among the worst natural disasters of the world, and resulted in 450,000 and 325,000 deaths, respectively (Ahmadalipour and Moradkhani, 2018a; Vicente-Serrano et al., 2012). The 2010–2011 drought in the Greater Horn of Africa affected >12 million people and resulted in massive migration, extreme famine, and mortality of over 260,000 people (Checchi and Robinson, 2013; Naumann et al., 2014a; Nicholson, 2014).

Drought risk refers to the potential losses from a particular hazard imposed by a drought event (Brooks et al., 2005; Cardona et al., 2012). In other words, drought risk is determined not only by the intensity of the event and its exposure, but also by the vulnerability of the society at a given time (Birkmann, 2007; Carrao et al., 2016). Therefore, drought risk is generally characterized as a function of three primary components: (i) hazard; that is the possible future occurrence of drought, (ii) vulnerability; that is the susceptibility of exposed elements to the adverse effects of drought, and (iii) exposure; that is the population and assets affected by drought (Blauhut et al., 2015b; Han et al., 2016; Zscheischler et al., 2018).

Reactive approaches are still used for drought management in most parts of the world, which is commonly referred to as crisis management, responding to the impacts that have already occurred (Svoboda et al., 2015; Wilhite et al., 2014). Nevertheless, these approaches are known to be untimely and disintegrated, and thus, previous drought management attempts have usually been ineffective with a rise in the socioeconomic impacts of drought (Peterson et al., 2013; Sivakumar et al., 2014). The scientific consensus has pointed out the necessity to move from reactive to proactive risk management strategies (Birkmann et al., 2013; Fekete et al., 2014; Rossi and Cancelliere, 2013).

Climate change and anthropogenic global temperature rise will pose significant impacts on natural hazards, extreme events, economy, and health (Ahmadalipour and Moradkhani, 2018b; Gergel et al., 2017; Honda et al., 2014). Multitude of studies have investigated the impacts of climate change on drought in various parts of the globe (Cheng et al., 2015; Zhao and Dai, 2017). It has been concluded that climate change will intensify drought hazard in many regions across the world (Ahmadalipour et al., 2017b; Cheng et al., 2015). This is especially more considerable in arid and semi-arid regions as global warming will in general increase the potential evapotranspiration (Asadi Zarch et al., 2014; Touma et al., 2015).

Besides the impacts of climate change, population growth is also expected to augment natural resources scarcity and food insecurity in Africa (Godfray et al., 2010; Khan et al., 2014; Seto et al., 2012). Population growth affects drought risk both directly, i.e. through increasing the exposure component of the risk, and indirectly, i.e. by aggravating drought vulnerability. Increasing population will demand additional resources of food, energy, and water for sustainable growth. Knowing that drought can significantly affect agriculture, energy, and water supply (Cai et al., 2018; Lobell et al., 2014; Xie et al., 2018), raising population will directly increase the risks of drought due to the increasing demand. In addition, increasing population can have negative impacts on measures of social vulnerability. For instance, exceptional periodic population growth in some of the countries in the past usually eventuated in high unemployment rates a few decades later, which consequently had negative impacts on their economy (Buhaug and Urdal, 2013). The considerably high population growth rate has become a grand challenge in Africa, especially for the least developed countries with limited resources, and it will be a substantial burden for social and human development (Antwi-Agyei et al., 2012; Hanjra and Qureshi, 2010).

Despite increasing concerns about the escalating impacts of droughts on food, energy, and water resources, it has been argued that more attention has been given to studying drought hazard rather than providing consistent drought risk assessment frameworks (Kim et al., 2015; Shiau and Hsiao, 2012; Tánago et al., 2016). In fact, many of the recent studies that claim to assess "drought risk" have actually studied the probability of drought hazard, ignoring the vulnerability and exposure components of risk (e.g. Cheng et al., 2015; Cook et al., 2015; Diffenbaugh et al., 2015).

The combination of climate change, population growth, and the aggravation of socioeconomic vulnerabilities in many regions of Africa will intensify drought hazard, exposure, and vulnerability, respectively. Therefore, it is important to investigate the changes of each component of risk separately and understand their integrated impacts on drought risk. The current study is among the first multi-dimensional assessments of compound effects of climate change, population growth, and vulnerability on drought risk across Africa. Drought risk is investigated at a national level for the historical as well as future periods, and its decadal changes are investigated for each country. The risk ratio is calculated for each country for different scenarios, and it is then decomposed to reflect the role of each component. In addition, the uncertainty raised by various sources is characterized, and its spatial and temporal patterns are investigated. The results provide long-term projections of drought risk ratio and reveal the role of each component (i.e. hazard, vulnerability, and exposure) on drought risk of each country, and will attribute the associated uncertainties.

2. Data and methods

The risk formulation employed in this study is the same as that implemented by the United Nations International Strategy for Disaster Reduction (UNISDR, 2015) and the Intergovernmental Panel on Climate Change (IPCC, 2012), and it has been utilized in multitude of earlier assessments (Cardona et al., 2012; Carrao et al., 2016; Peduzzi et al., 2009, 2002). It is defined as:

$$Risk = Vulnerability \times Hazard \times Exposure \quad (1)$$

Therefore, three different types of data are utilized to address the three components of risk (i.e. hazard, vulnerability, and exposure) as explained in the following sections.

2.1. Vulnerability

In order to quantify drought vulnerability, 28 factors from six different sectors of land use, economy, health, energy and infrastructure, social, and water resources were acquired from two primary resources: Food and Agricultural Organization (FAO) of the United Nations and the World Bank. The data for each factor was quality controlled and normalized, and after several statistical analyses (presented in Supplementary Fig. S1) including multi-collinearity test, weighted averaging, change-point analysis, and cluster analysis, a composite Drought Vulnerability Index (DVI) was calculated for each country (Ahmadalipour and Moradkhani, 2018a). The calculated DVI ranges between 0 and 1 corresponding to the lowest and highest vulnerability, respectively.

Table 1
The 10 RCMs used in this study and their characteristics. All the RCMs were developed by the Swedish Meteorological and Hydrological Institute (SMHI) and have a spatial resolution of 0.44°.

No.	Deriving GCM	Original modeling institute	Original resolution (lat × lon)	Ens. member
1	CanESM2	Canadian Centre for Climate Modeling and Analysis	2.8° × 2.8°	r1i1p1
2	CNRM-CM5	National Centre of Meteorological Research, France	1.4° × 1.4°	r1i1p1
3	CSIRO-Mk3-6-0	Commonwealth Scientific and Industrial Research Organization, Australia	1.8° × 1.8°	r1i1p1
4	EC-EARTH	EC-EARTH consortium	1.0° × 1.0°	r12i1p1
5	GFDL-ESM2M	Geophysical Fluid Dynamics Laboratory	2.5° × 2.0°	r1i1p1
6	HadGEM2-ES	Met. Office Hadley Centre	1.88° × 1.25°	r1i1p1
7	IPSL-CM5A-MR	Institut Pierre-Simon Laplace	2.5° × 1.25°	r1i1p1
8	MIROC5	Atmosphere and Ocean Research Institute (The University of Tokyo), National Institute for Environmental Studies, and Japan Agency for Marine-Earth Science and Technology	1.4° × 1.4°	r1i1p1
9	MPI-ESM-LR	Max Planck Institute for Meteorology (MPI-M)	1.9° × 1.9°	r1i1p1
10	NorESM1-M	Norwegian Climate Centre	2.5° × 1.9°	r1i1p1

The multi-dimensional DVI was calculated during the historical period of 1960–2015, and then considering the long-term historical variations and trends of DVI for each country, three future DVI scenarios (low, medium, and high vulnerability) were statistically projected (extrapolated) for 2020 to 2100. Various assessments and evaluations were carried out to ensure the reliability and accuracy of the calculated DVI. More details about the factors and data availability for each country is presented in Supplementary information, and the vulnerability assessment is thoroughly explained in Ahmadalipour and Moradkhani (2018a).

2.2. Hazard

For assessing drought hazard, Regional Climate Models (RCMs) developed by the Coordinated Regional Climate Downscaling Experiment (CORDEX) are utilized for the African domain, i.e. AFR-44 which covers the boundary of [−45.76°S–42.24°N] and [−24.64°W–60.28°E] (Jones et al., 2011). Previous studies evaluated CORDEX RCMs across various regions considering different variables, and found reasonable performance in most regions (Diasso and Abiodun, 2017; Kim et al., 2014; Nikiema et al., 2017; Önol et al., 2013; Ring et al., 2017). Here, precipitation (Prec) and potential evapotranspiration (PET) are acquired from 10 RCMs at a daily timescale and 0.44° spatial resolution (about 40 km) for the entire African continent during the historical period of 1951–2005 as well as two future emission scenarios of RCP4.5 (representing moderate emission increase and corresponding to 2 °C mean global warming by the end of the 21st century) and RCP8.5 (business as usual scenario) for the period of 2006–2100. The daily data are then aggregated to monthly timescale to be employed for drought analysis. More information about the RCMs used in this study is presented in Table 1.

In this study, drought hazard is quantified using the Standardized Precipitation Evapotranspiration Index (SPEI) (Vicente-Serrano et al., 2010). SPEI is a multi-scalar drought index that accounts for temperature effects on drought and it has been employed in numerous studies (Chen and Sun, 2017; Li et al., 2015; Naumann et al., 2014b). It is based on a climatic water balance and considers water deficit as the difference between precipitation and potential evapotranspiration (D = P − PET). The water deficit (D) can be calculated at different accumulation periods to reflect the variations at different timescales. In this study, D is calculated for each grid cell (at 0.44-degree spatial resolution) and each month, and then accumulated to 12-month timescale in order to capture the long-term impacts of climate change as suggested by previous studies (Ahmadalipour et al., 2017a). The nonparametric Weibull plotting position is utilized to calculate the SPEI as follows:

$$P(X_i) = \frac{i}{n+1} \tag{2}$$

where i is the rank of D from smallest to largest, n is the sample size, and $P(X_i)$ denotes the empirical probability. $P(X_i)$ is then transformed to the standard normal distribution (with zero mean and unit standard deviation) which will be the corresponding value of the SPEI:

$$SPEI = \varnothing^{-1}(P) \tag{3}$$

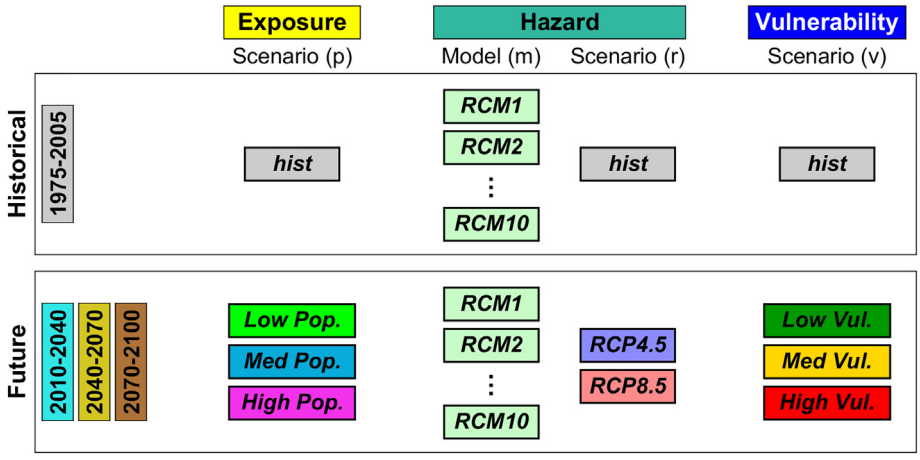

Fig. 1. Schematic diagram of the risk analysis methodology employed in this study and its different components in historical and future periods. The method is implemented separately for each of the 46 African countries, and risk ratio is calculated for each scenario. The colors used in this figure for each component are consistent throughout the manuscript.

A zero value for SPEI corresponds to no drought condition, and negative values represent an imbalance in the available water, indicating drought condition. The lower the value of SPEI, the higher is the intensity of drought.

The SPEI is calculated separately for each month, and the monthly values are then aggregated to obtain the time-series of drought index. The methodology is employed for each grid cell of each RCM for the historical period of 1951–2005 and two future emission scenarios of RCP4.5 and RCP8.5 during 2006–2100. A *Hazard Index* is then calculated to quantify drought hazard at national scale in each year. Drought hazard of a particular month for a country is obtained by averaging the negative SPEI values across the country and dividing it by the total number of grids of that country. Then, the annual drought hazard will be the mean of monthly drought hazards (during dry months) as follows:

$$Hazard\ Index = \left| \sum_{i=1}^{12} \sum_{n=1}^{N_i} SPEI_{i,n}(<0)/12G \right| \quad (4)$$

where i indicates the month, N_i denotes the number of grids in the country that experience drought in month i, and G is the number of grids that cover the country. Hazard Index is calculated separately for each country and each model. The drought hazard calculated by the above function will have the same absolute range as the SPEI (in this case, $0 <$ *Hazard Index* $<$ ~2.2). It reflects the overall severity of drought in a year for a particular region. For instance, if half of a country (i.e. $\frac{N}{G} = 0.5$) experiences moderate drought (SPEI $= -1$) for 6 months in a year and no drought for the rest of the year, the calculated Hazard Index will be 0.25 ($1 \times 0.5 \times \frac{6}{12} = 0.25$). The maximum Hazard Index is observed when the entire region experiences extreme drought (SPEI < -2) for the entire year. Therefore, the proposed Hazard Index is a compound indicator of the intensity, duration, and extent of drought.

Apart from the national-scale Hazard Index, two important characteristics of drought hazard are also investigated at the grid-scale (0.44° spatial resolution): the spatial extent of drought and trends of drought intensity. Drought extent is calculated by detecting the area (i.e. number of grid cells) that is affected by drought (i.e. SPEI

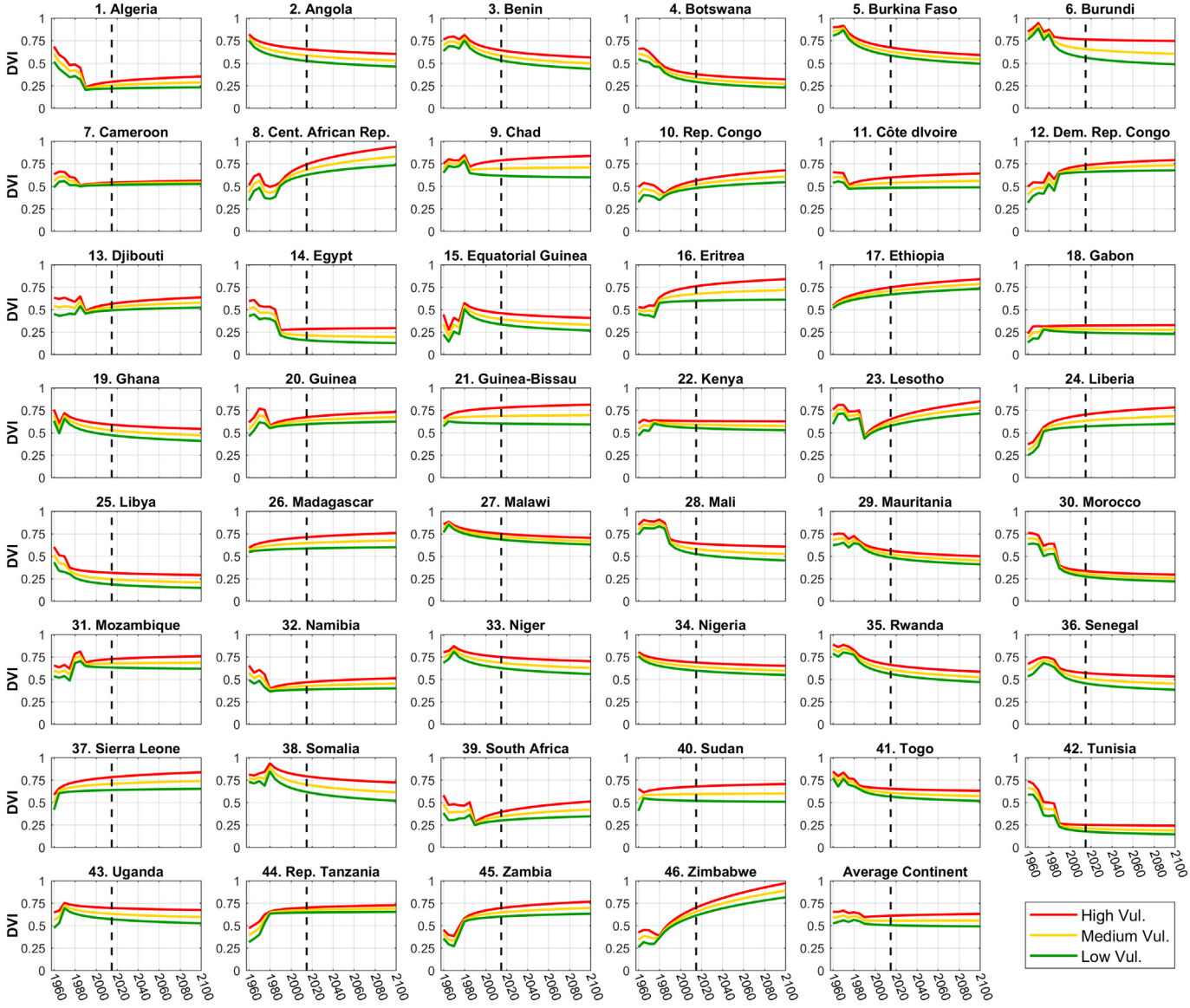

Fig. 2. Temporal variations of Drought Vulnerability Index (DVI) for each country during the historical period of 1960–2015 and future projections of 2020–2100. The last plot shows the average DVI among all 46 African countries in each scenario. The vertical dashed black lines divide between historical and future periods.

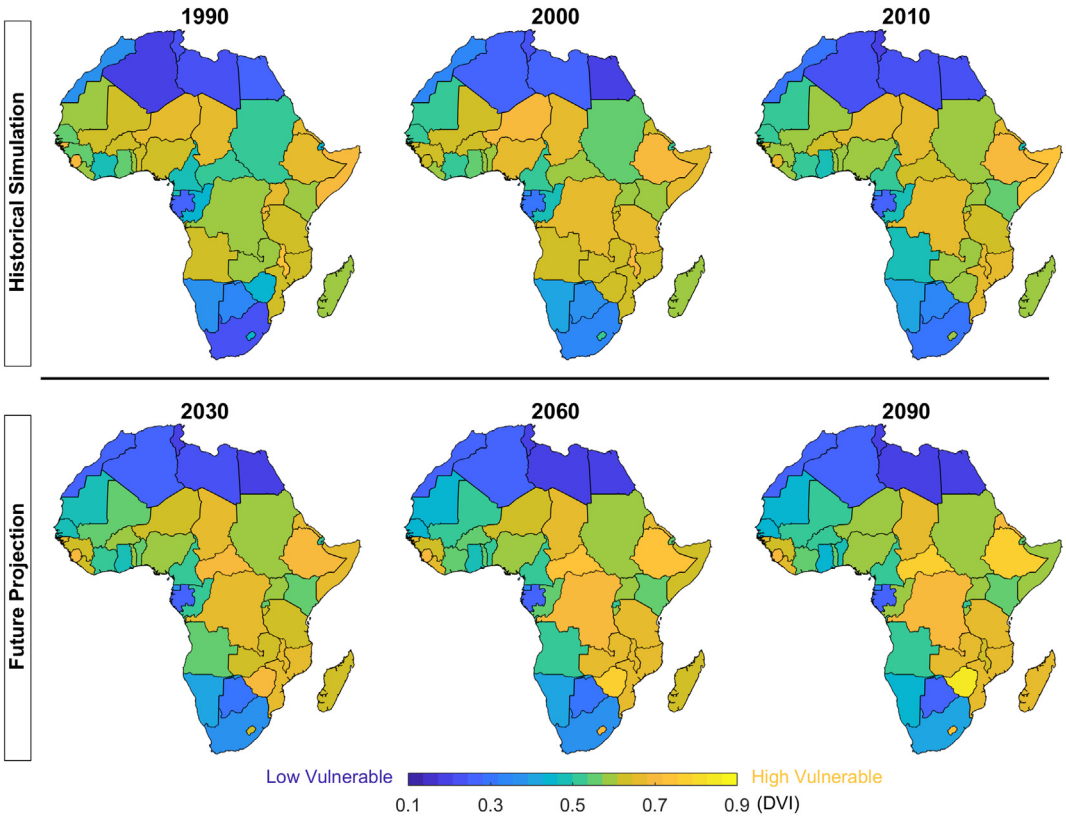

Fig. 3. Spatial variations of Drought Vulnerability Index (DVI) for historical simulations and future projections. The figure shows the results of medium vulnerability scenario for both historical and future periods.

< -0.8; Chen et al., 2012) divided by the total area of the African continent. Moreover, the long-term linear trends of drought intensity are assessed for each grid during the future period of 2005–2100 (Ahmadalipour et al., 2017b). The Mann-Kendall trend test, as a rank-based non-parametric test and independent of the statistical distribution, is utilized to investigate the significance of trends (Kendall, 1948).

2.3. Exposure

Exposure is investigated using human population data for each African country. The population data are acquired from United Nations (2015) and utilized for the historical period of 1950–2015 as well as three future population projection scenarios of low, medium, and high variant population scenarios over the period of 2015–2100.

2.4. Drought risk

After quantifying hazard, vulnerability, and exposure for each country, drought risk is also quantified at a national scale. For each country, drought risk is quantified for the historical period of 1975–2005, and the historical mean drought risk is calculated for each RCM. This 30-year period is chosen since it provides more accurate data compared to antecedent years (especially the socio-economic data that are utilized for drought vulnerability). Similar procedure is implemented to calculate drought risk projections of near future (2010–2040), intermediate future (2040–2070), and distant future (2070–2100). After calculating drought risks for historical and future periods, the changes of drought risk in each country are assessed by comparing the projected risk scenarios with the simulated historical drought risk. Risk ratio is calculated for each country by multiplying the change rate of hazard, exposure, and vulnerability as follows:

$$Risk\ Ratio_{m,r,p,v} = \frac{Risk_{fut;m,r,p,v}}{Risk_{hist;m}} = \frac{Hazard_{fut;m,r}}{Hazard_{hist;m}} \times \frac{Exposure_{fut;p}}{Exposure_{hist}} \times \frac{Vulnerability_{fut;v}}{Vulnerability_{hist}} \quad (5)$$

where *hist* and *fut* indicate historical and future periods, respectively. *m*, *r*, *p*, and *v* denote different permutations of climate models (RCMs), climate scenarios (RCPs), population scenarios, and vulnerability scenarios, respectively. The risk ratio is calculated for each country for three future periods (i.e. 2010–2040, 2040–2070, and 2070–2100). Fig. 1 shows a schematic diagram of drought risk components utilized in this study during historical and future periods.

Beside the country-level risk ratio analyses, the changes of each risk component are also investigated along with the overall changes of drought risk ratio over the continent. Overall, drought risk ratios are quantified for each African country (46 countries) for 10 RCMs, 2 climate scenarios (RCP4.5 and RCP8.5), 3 vulnerability scenarios (low, medium, and high vulnerability), and 3 population scenarios (low, medium, and high population) during three 30-year future periods (near, intermediate, and distant future), totaling 24,840 drought risk permutations/scenarios across the continent ($46 \times 10 \times 2 \times 3 \times 3 \times 3 = 24{,}840$). The large ensemble of models and scenarios employed in this study makes it possible to probabilistically assess future drought risk changes and characterize the uncertainties associated with different sources.

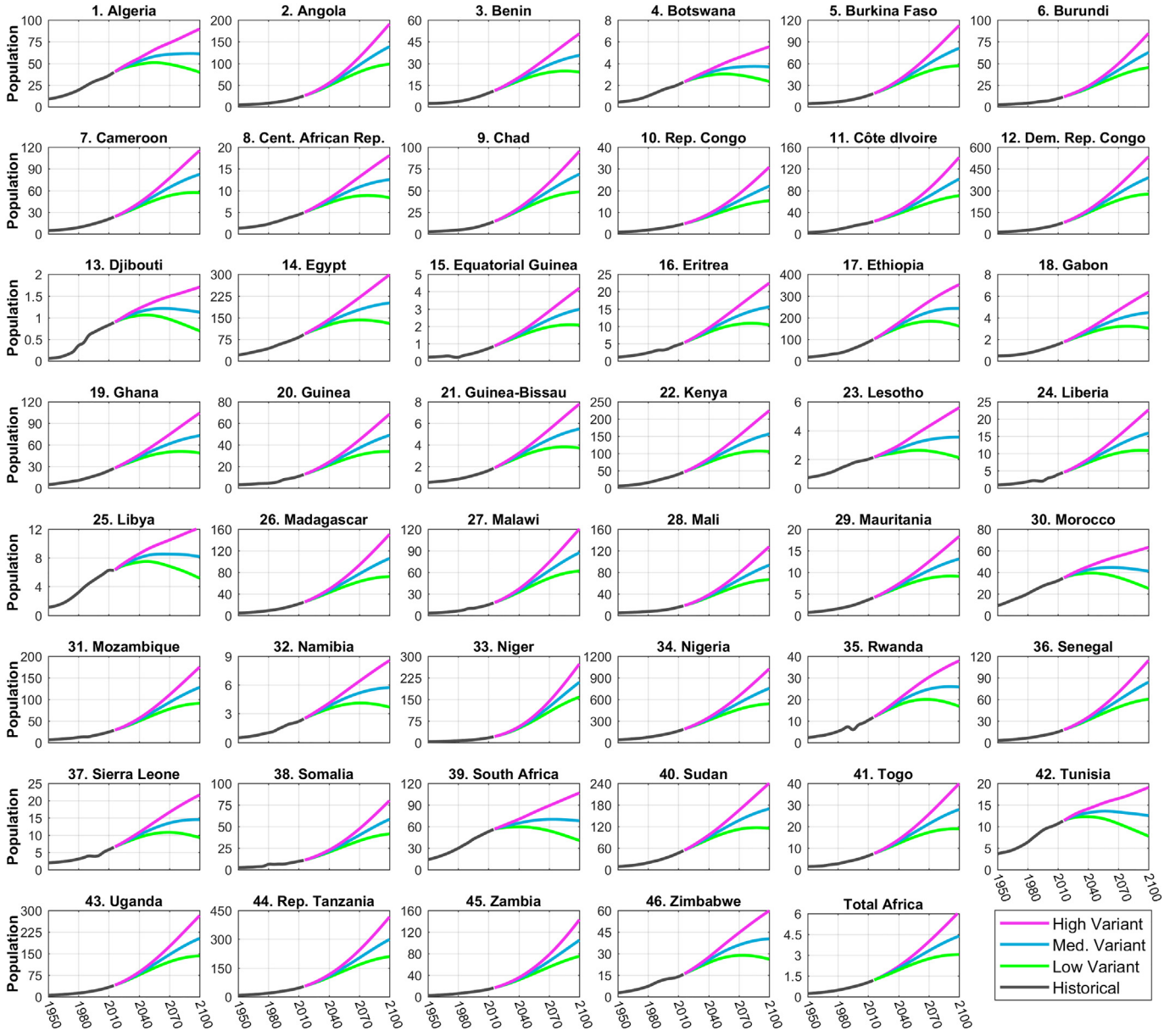

Fig. 4. Historical record and projected population of each country in the African continent. The last subplot shows the total population of the African continent. The y-axis in all subplots is in million people, except for the last subplot (Total Africa) which presents the population in billions.

2.5. Characterizing uncertainties

Applying the methodology for different models/scenarios, a total of 180 risk ratios (10 climate models × 2 climate pathways × 3 vulnerability scenarios × 3 population scenarios) are obtained for each country in each future period. It is essential to characterize the uncertainties associated with each source and understand their changes through time. Several previous analyses have examined various sources of uncertainty (e.g. model, scenario, downscaling, internal variability, model parameterization, or a combination of these) in climate change projections (Chen et al., 2011; Hawkins et al., 2015; Hawkins and Sutton, 2011; Jung et al., 2012; Mizukami et al., 2016). The current study follows similar approach and builds up on the previous assessments by attributing uncertainty sources of hazard as well as vulnerability and exposure.

The fraction of total variance for each source of uncertainty is calculated in each country for each period. This is performed by calculating the normalized coefficient of variation of risk ratio acquired from different scenarios. Let $[R_1, R_2, \ldots, R_{180}]$ represent the ensemble of risk ratios of a particular country in a particular future period, and assume that $[R_1, \ldots, R_{90}]$ and $[R_{91}, \ldots, R_{180}]$ correspond to risk ratios for RCP4.5 and RCP8.5 climate scenarios, respectively. The average risk ratio will be calculated as $\mu_{all} = \frac{R_1+\ldots+R_{180}}{180}$. The mean risk ratios for each climate scenario will then be calculated as $\mu_{RCP4.5} = Avg(R_1, R_2, \ldots, R_{90})$ and $\mu_{RCP8.5} = Avg(R_{91}, R_{92}, \ldots, R_{180})$. Then, the standard deviation of RCP risk ratios will be derived by $\sigma_{RCP} = std(\mu_{RCP4.5}, \mu_{RCP8.5})$. σ_{RCP} will then be divided by μ_{all} to obtain the coefficient of variation ($CV_{RCP} = \sigma_{RCP}/\mu_{all}$) in order to normalize the variance among different countries and different periods, which makes them comparable. Similar procedure is implemented to calculate CV_{Model}, CV_{Vul}, and CV_{Pop}. Then, for each country, the fraction of total variance (FTR) for each component reflects the relative contribution of the uncertainty source to the total variance (i.e. $FTR_{RCP}(\%) = \frac{CV_{RCP}}{CV_{Model}+CV_{RCP}+CV_{Vul}+CV_{Pop}} \times 100$).

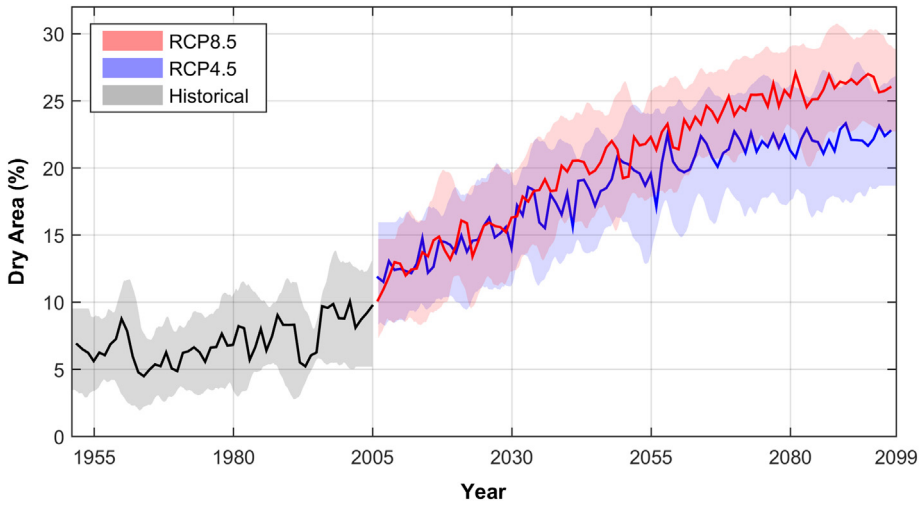

Fig. 5. Spatial extent of drought across Africa based on the SPEI-12 results for historical and future periods. The shaded area represents the results of 10 RCMs and the lines indicate the ensemble mean dry area for each corresponding emission scenario.

3. Results and discussion

3.1. Drought vulnerability

Drought vulnerability analyses and projections are thoroughly and exclusively explained in Ahmadalipour and Moradkhani (2018a). Fig. 2 shows the Drought Vulnerability Index (DVI) calculated for each country during the historical period of 1960–2015 and projected to the future period of 2020–2100. Considering the medium DVI scenario (shown in yellow), the number of countries indicating decreasing, increasing, and no considerable future DVI trends are 19, 13, and 14, respectively. Focusing on the late 21st century, Egypt and Tunisia indicate the lowest DVIs, and Central African Republic and Zimbabwe show the highest drought vulnerability. In order to better understand the spatial patterns of DVI, the results of medium DVI scenario are plotted in Fig. 3 for 1990, 2000, and 2010 in the historical period and 2030, 2060, and 2090 in future projections. Fig. 3 shows that, in general, northern African countries (i.e. Egypt, Libya, Tunisia, and Algeria) have the lowest DVI in most years followed by southern African countries. Whereas, the countries located in central Africa indicate higher drought vulnerability. For instance, Somalia and Ethiopia (located at the horn of Africa) indicate the highest drought vulnerability in 2010, which resulted in extremely high fatalities following the 2011 drought in the region (Lyon, 2014; Nicholson, 2014).

3.2. Exposure

Fig. 4 shows the annual population projection of each country during the historical period (shown in grey) and three future scenarios of low, medium, and high variant population (shown in green, blue, and purple, respectively, consistent with Fig. 1). In general, all African countries are expected to experience vast expansion in their population in the upcoming decades. The substantial population increase is more pronounced for Total Africa (the last subplot in Fig. 4). The population of Africa was about 1 billion people at the end of the 20th century, whereas it will increase to 3, 4.5, and 6 billion people by the end of the 21st century for low, medium, and high variant population scenarios, respectively. This unprecedented population will impose serious challenges for Africa regarding social development, food security, health, and many other sectors (Gerland et al., 2014; Schlosser et al., 2014; Vörösmarty et al., 2000). The most population increase rate is found in Niger and Chad (neighboring countries located at the sub-Saharan region), both of which are among the highly vulnerable countries in terms of social and human development sectors (Ahmadalipour and Moradkhani, 2018a; Neumayer, 2001). For instance, Niger's population was about 10 million people in the 2000s, and it is expected to increase to 150–250 million people by 2090s. Considering the limited economic and natural resources of the country due to its geopolitical location and the arid climate of the region, this demographic growth will lead to substantial drought risks. On the contrary, Libya, Morocco, and Tunisia (all of which are located at the northern parts of the African continent) show the least population change, and even indicating decreasing population for the low variant scenario, which are also among the least drought vulnerable countries in Africa (Ahmadalipour and Moradkhani, 2018a).

3.3. Drought hazard

Fig. 5 shows the spatial extent of drought across the African continent calculated from the SPEI-12 results for the historical period (shown in grey) as well as two future scenarios of RCP4.5 and RCP8.5 (shown in blue and red, respectively). The shaded area indicates ± 1 standard deviation of the results of 10 RCMs, and the lines represent the ensemble mean drought extent for the corresponding scenario. The figure shows that mean drought extent over Africa is about 7% in the historical period, and it increases to about 25% by late 21st century. Slightly increasing drought extent is detected during the historical period, especially after 1990s. The drought extent projections of RCP4.5 and RCP8.5 are similar until the 2030s, with the latter showing higher dry area afterwards.

The long-term future trends of SPEI-12 are calculated for each RCM during the period of 2005–2100, and the results are shown in Fig. 6. The figure shows the mean decadal change of SPEI for RCP4.5 (top) and RCP8.5 (bottom). A negative trend value indicates decreasing SPEI and thus increasing intensity of drought. The Mann-Kendall trend test is utilized to investigate the significance of trends at 0.05 significance level, and only the negative trends (intensifying drought conditions) that are significant (with a p-value < 0.05) are plotted in Fig. 6. Most of the RCMs indicate significantly increasing drought intensity for northern and southern parts of Africa. It should be noted that a decadal trend value of -0.2 (shown in red color) leads to substantial increase of drought intensity, as it means that in 25 years (2.5 decades) the average SPEI value will decrease by 0.5 ($-0.2 \times 2.5 = -0.5$). It implies that drought intensity is expected to be exacerbated by one class, given the SPEI thresholds of -1, -1.5, and -2 representing moderate, severe, and extreme drought conditions, respectively (Ahmadalipour et al., 2017b; Dai, 2012). In general, results of both RCPs show similar spatial patterns, and RCP8.5 indicates more intense droughts than RCP4.5. For

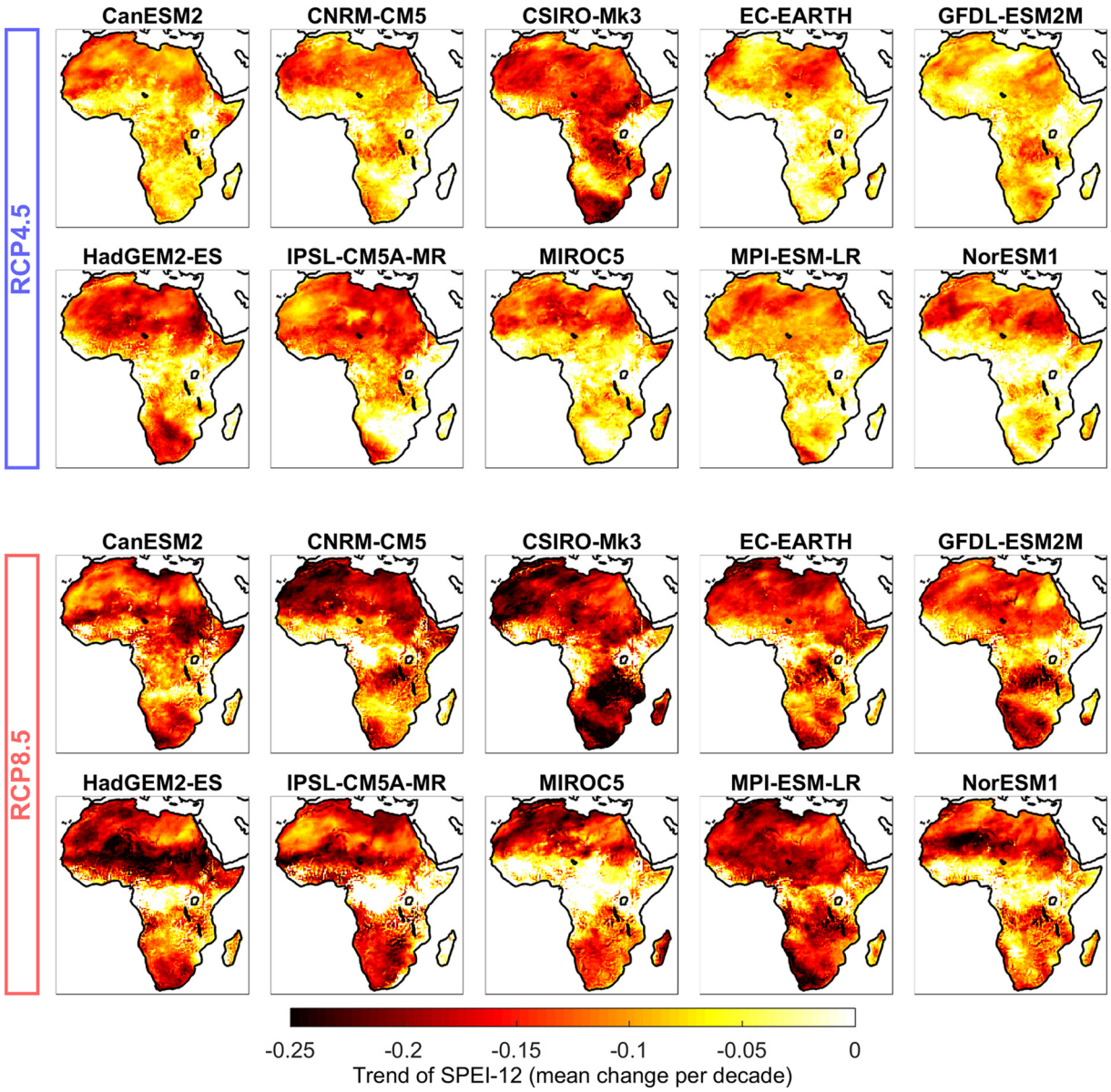

Fig. 6. Long-term trend of SPEI-12 during the future period of 2005–2100 for each RCM in RCP4.5 (top) and RCP8.5 (bottom). The Mann-Kendall trend test is used at 0.05 significance level and only the significantly negative trends are plotted.

instance, the RCP4.5 models show trend values of less than −0.15 in most regions, whereas results of RCP8.5 indicate trends twice as much in many regions. The results of Fig. 6 are in agreement with previous assessments using other drought indices such as the Palmer Drought Severity Index (PDSI) (Dai, 2012; Zhao and Dai, 2017), Supply–Demand Drought Index (SDDI) (Touma et al., 2015), and Reconnaissance Drought Index (RDI) (Asadi Zarch et al., 2014).

The Hazard Index (Eq. (4)) is calculated for the 10 RCMs in each country during the historical and future periods. Fig. 7 shows the temporal changes of Hazard Index and the associated model and scenario uncertainties. The historical, RCP4.5, and RCP8.5 results are plotted in grey, blue, and red, respectively, with the shaded area showing the results of 10 RCMs (±1 standard deviation) and the lines representing the ensemble mean. The projections of Hazard Index show different patterns and diverse uncertainties for different countries. In general, the northern African countries (i.e. Algeria, Egypt, Libya, Morocco, and Tunisia) indicate increasing Hazard Index during the historical period, all of which demonstrate aggravating future Hazard Index as well. The countries located at southern parts of Africa (i.e. Botswana, Namibia, South Africa, and Mozambique) follow similar patterns, but with less intensity. On the contrary, the western African countries below the Sahel region (i.e. Côte d'Ivoire, Guinea, Liberia, and Sierra Leone) do not indicate any significant changes in Hazard Index for neither the historical period nor future projections, and the Hazard Index of the two future scenarios are similar for these countries. For other countries, RCP8.5 indicates higher Hazard Index than RCP4.5. The worst drought hazard conditions are expected to happen in Egypt and Libya. Egypt is also the country with the lowest model uncertainty (the narrowest shaded area) especially for RCP8.5 emission scenario that almost all RCMs indicate substantially intensifying Hazard Index. In general, the median Hazard Index among 46 African countries is below 0.5 during the historical period, and it is projected to become twice as much in distant future.

To better understand the spatial patterns associated with projected drought hazard, the hazard ratio (future Hazard Index divided by historical Hazard Index) of each country is calculated for the ensemble mean of the 10 RCMs, and the results are shown in Supplementary Fig. S3. The figure shows that drought hazard is expected to substantially exacerbate in the northern parts of Africa, and the northern African countries

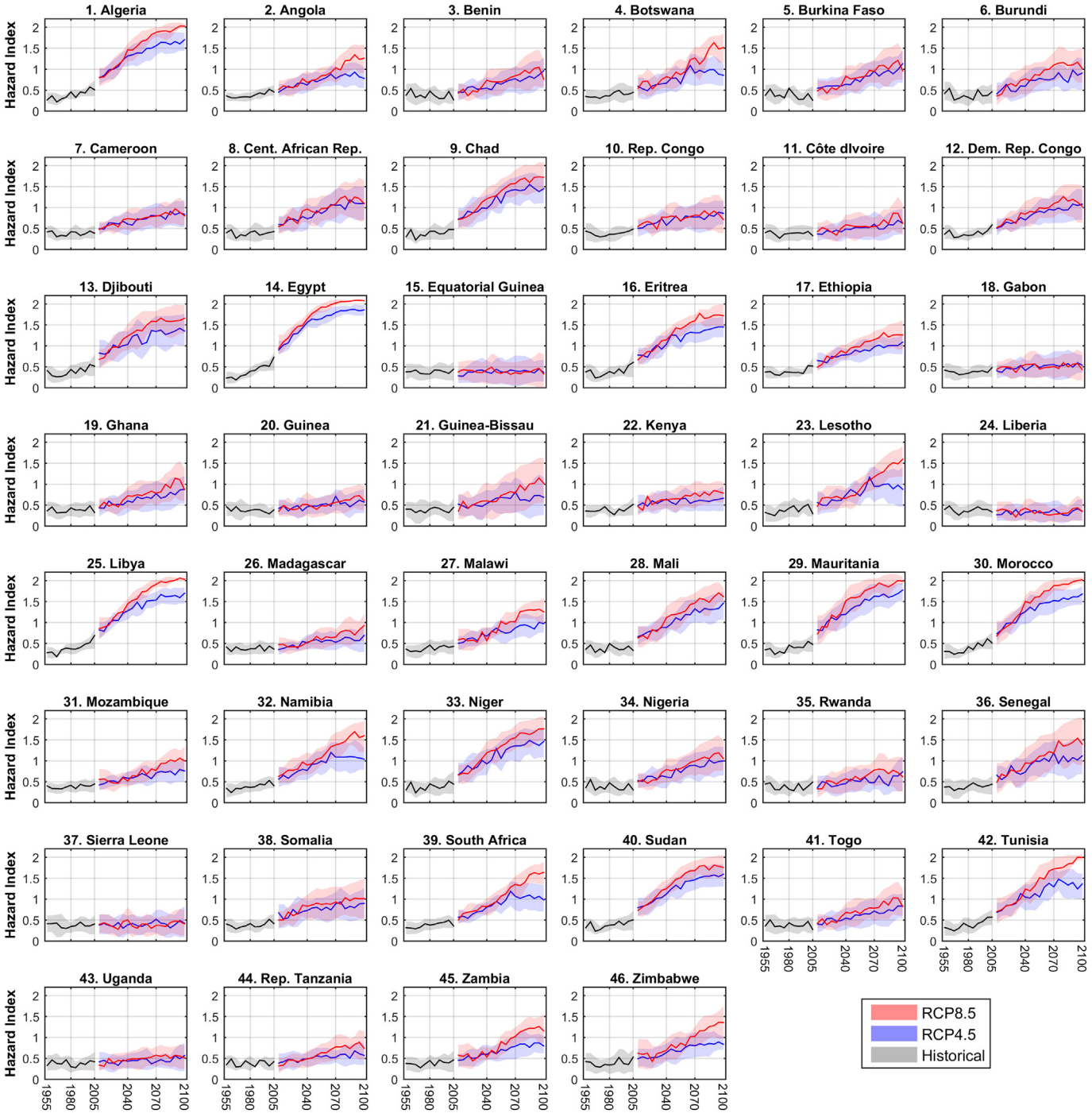

Fig. 7. Temporal variations of the annual Hazard Index for each country in Africa during the historical period as well as two future emission scenarios of RCP4.5 and RCP8.5. The shaded areas represent the results of 10 climate models and the lines indicate the ensemble mean.

indicate fourfold drought hazard in the distant future (compared to the historical period).

3.4. Drought risk

Drought risk ratio (Eq. (5)) is calculated for each country for all models and climate/population/vulnerability scenarios during the future periods of 2010–2040, 2040–2070, and 2070–2100. The risk ratios for all scenarios in near and distant future are shown in Supplementary Fig. S3. The figure shows that risk ratio from different scenarios are similar in near future, whereas large differences are found among risk ratios of various scenarios in distant future. Therefore, drought risk ratio of the ensemble mean of 10 RCMs during 2070–2100 is shown in Fig. 8 for all climate, population, and vulnerability scenarios. From Fig. 8, the central African countries (e.g. Niger, Chad, Sudan, and Democratic Republic of Congo) indicate higher risk ratios compared to the southern and northern African countries. The spatial patterns are somehow similar to those for drought vulnerability in Africa (Ahmadalipour and Moradkhani, 2018a; Naumann et al., 2014a). In general, the southern and northern African countries are more developed, with access to

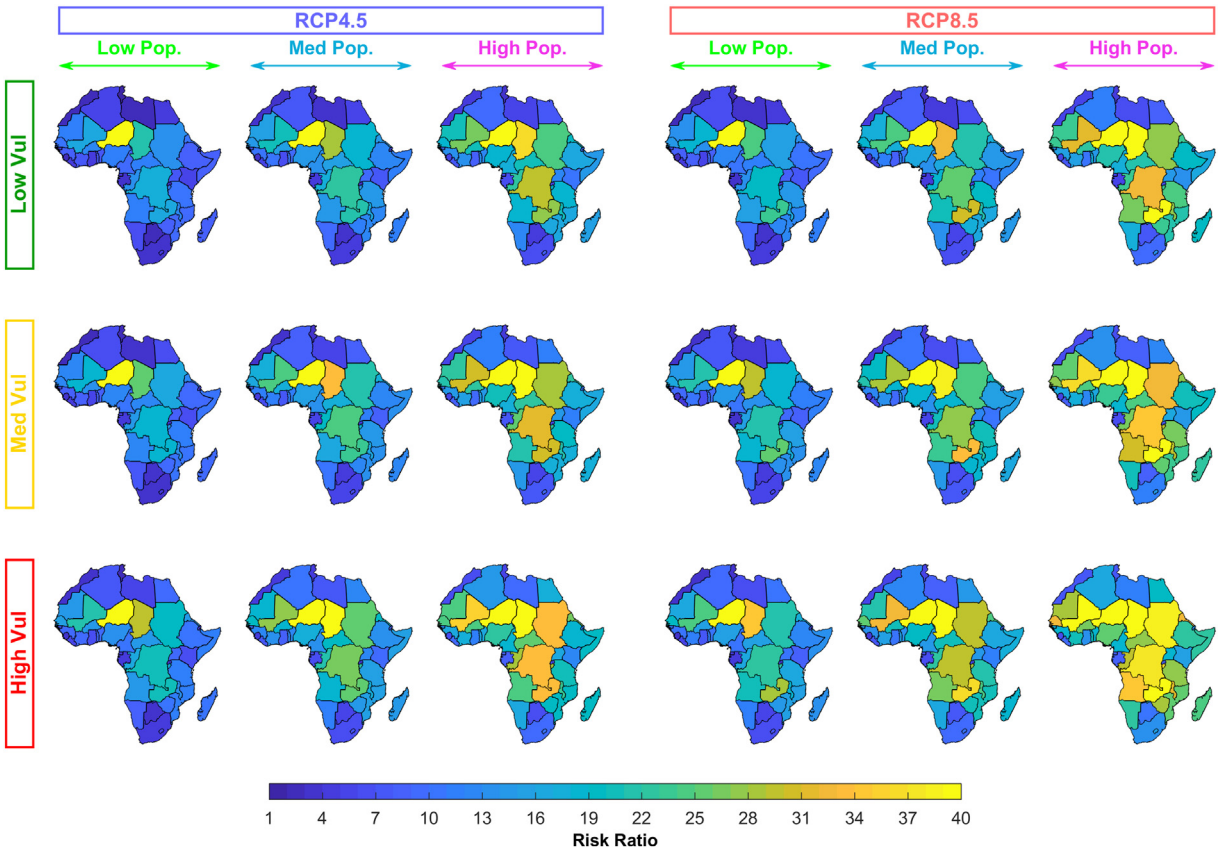

Fig. 8. Projections of the ensemble mean (of 10 RCMs) drought risk ratio in different scenarios: two climate scenarios (RCP4.5 and RCP8.5), three population scenarios (Low, Medium, and High population), and three vulnerability scenarios (Low, Medium, and High) in distant future (2070–2100).

more resources and thus indicating lower socioeconomic vulnerabilities and higher social development. This is in turn influential on their future population projections, keeping the exposure at mediocre levels for the majority of developed countries, and consequently yielding lower risk ratios (Gerland et al., 2014). Fig. 8 presents the results for 2070–2100, and the results for 2010–2040 and 2040–2070 are shown in Supplementary Figs. S4 and S5, respectively.

In order to better understand the risk ratio differences among various periods and to explore model uncertainties, the distribution of risk ratio from 10 climate models is shown in Supplementary Fig. S6 for medium vulnerable scenario in both climate scenarios as well as low and high population scenarios in all future periods. The figure shows that the lowest risk ratio is found in Tunisia, Morocco, and Libya, respectively, all of which are located in northern Africa. Despite the substantial increase of drought hazard in these three countries, they all indicate decreasing vulnerability and low changes in exposure. For instance, the exposure is expected to decrease in these countries in low population scenario. Nonetheless, the drought risk in distant future is expected to become at least 2–3 times higher than that during historical period. On the contrary, Niger and Chad demonstrate the highest risk ratios. The combination of high emission scenario and high variant population scenario (*High Pop.* & *RCP8.5*) in 2040–2070 can lead to risk ratios as large as a moderate scenario (*Low Pop.* & *RCP4.5*) in 2070–2100. In other words, if no adaptation/mitigation planning is carried out for climate emissions and population, the devastating risks are accelerated to happen decades earlier.

The distribution of risk ratio among 46 African countries is plotted in Fig. 9 for each future period/scenario to investigate the overall drought risk ratio across the African continent. The median drought risk ratio in near future is about 4, whereas it increases to about 9 in intermediate future, and ranges between 10 and 20 in distant future. The difference between various scenarios is negligible in near future, whereas disparities are found among them in distant future. In distant future (third row), the highest risk ratio of the optimum (most favorable) scenario (i.e. *Low Vul*, *Low Pop*, and *RCP4.5*) is about the same as the median of the worst-case scenario (i.e. *High Vul*, *High Pop*, and *RCP8.5*), which reflects the importance of adaptation and resources planning and management, especially in distant future.

3.5. Decomposing drought risk components

Results indicated that the role of each drought risk component is different among various countries. In some countries (e.g. Niger), population increase seems to be the main issue for aggravating drought risk. Since the drought risk formulation integrates hazard, vulnerability, and exposure, it is necessary to decompose risk and assess the role of each component. Fig. 10 shows the change rate of each component of risk in each country for near and distant future. For instance, the change rate of vulnerability is calculated as $\frac{Vulnerability_{fut}}{Vulnerability_{hist}}$. The figure shows the ensemble mean change rate from the multitude of available scenarios for each component. In Fig. 10, the countries are arranged in descending order of drought risk ratio from the highest to lowest (it should be noted that the risk is obtained by multiplying the components, and not by adding them. Therefore, the stacked bars should not be viewed as additive rates, and their product matters for risk ratio). In each component, a change rate lower than 1 indicates a decreasing trend, which is in favor for decreasing drought risk. This is found to be true for vulnerability in several countries (e.g. Egypt, Morocco, and Tunisia) that vulnerability change rate is below 1. Focusing on hazard change rates, Liberia shows the lowest rate with a slightly decreasing hazard for both future periods, whereas all other countries show increasing hazard with varied ranges.

Fig. 10 identifies the differences between hazard and exposure change rates. For instance, in near future, most of the countries indicate

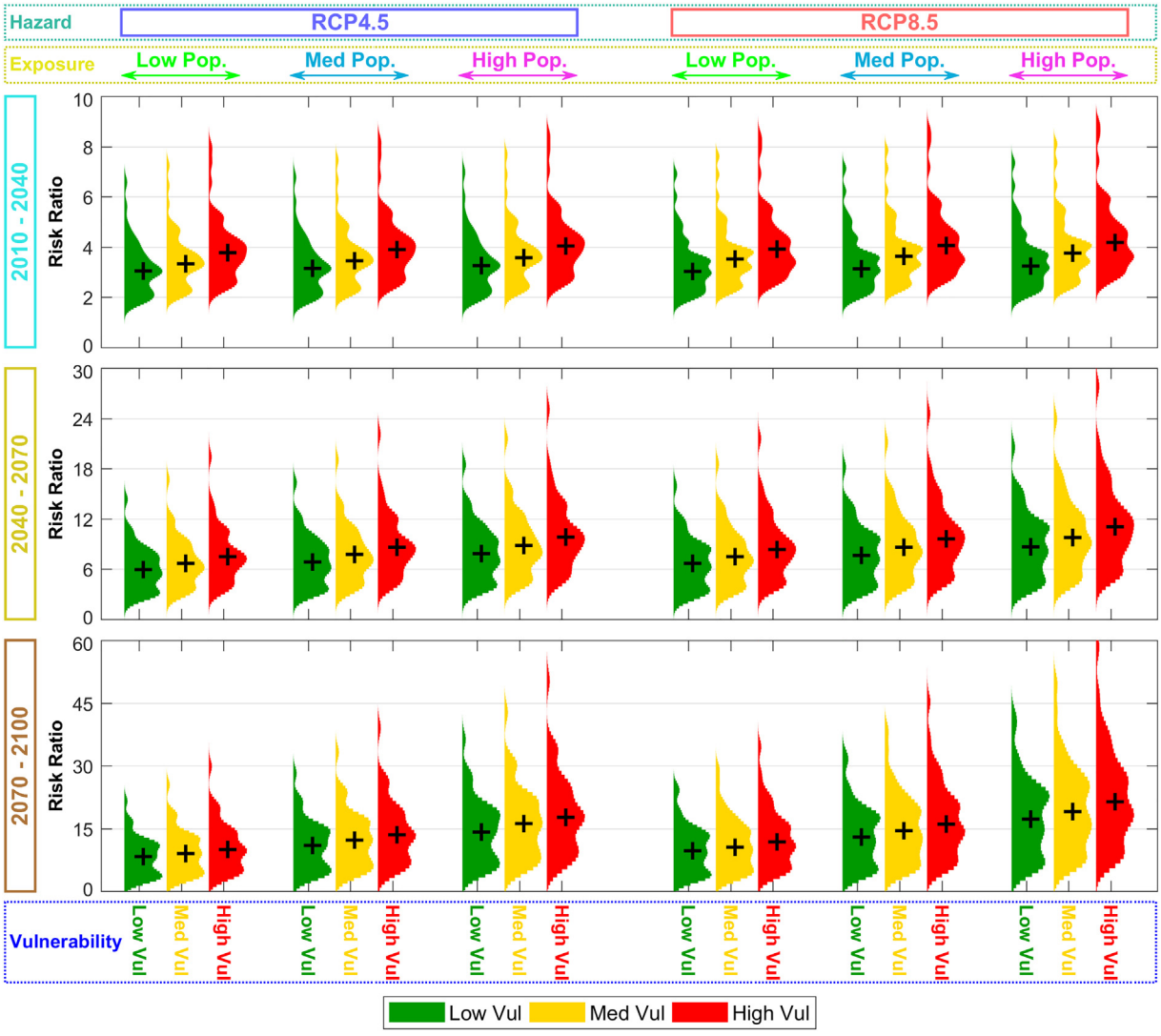

Fig. 9. Violin plots representing the distribution of the drought risk ratio among the 46 African countries for future periods/scenarios. The plus signs (+) indicate the median risk ratio in each case.

similar change rates for hazard and exposure, except for the northern African countries (i.e. Algeria, Egypt, and Morocco) where hazard change rates are higher than that of exposure, and the central African countries (i.e. Burundi, Equatorial Guinea, and Rwanda) where exposure change rates are greater than hazard change rates. In distant future however, the majority of countries indicate significantly higher change rates for exposure compared to hazard, which reflects the critical influence of population growth on drought risk. Comparing the overall ranking of countries in near and distant future, the top and low countries are the same in both periods. Djibouti shows the highest relative improvement of drought risk ratio from near future (ranked 36th among African countries) to distant future (ranked 13th). On the other hand, Burundi is ranked 26th in near future and it falls to rank 38th in distant future. In both of these countries, the changes of exposure has an important role in mitigating or aggravating the rank of drought risk ratio.

3.6. Uncertainty assessment

The fraction of total variance (explained in Section 2.5) is calculated for each uncertainty source in each country and each future period, and the results are shown in Fig. 11. From the figure, the main source of uncertainty in near future is vulnerability followed by climate models. Climate pathway and exposure seem to be least influential on risk ratios of near future. In fact, climate pathway seems to be the lowest source of uncertainty for drought risk in all future periods. It should be noted that the choice of climate pathway is critical for drought 'hazard' (as shown in Fig. 7) (Nangombe et al., 2018; Sheffield and Wood, 2008; Zhao and Dai, 2017). However, when compared with the other three uncertainty source of drought 'risk', climate pathway is found to be the least influential source of uncertainty.

To better understand the overall changes of uncertainty for different sources, distribution of the fractions of total variance among the 46 African countries is shown in Fig. 12 for each period. Fig. 12 shows that vulnerability is characterized with the highest uncertainty, followed by climate models as a major sources of uncertainty in drought risk analysis. The uncertainty raised by climate models indicates similar range in all periods (ranging around 20–50%) with similar variation among the countries (i.e. the width of boxplots for climate model is almost the same in the three periods). Whereas, the fraction of total variance for vulnerability decreases through time (with a median value of 55% and 35% for near and distant future, respectively), and it increases for exposure and climate pathway. In general, climate models were shown to be a major source of uncertainty in drought and climate change impact assessments (Ahmadalipour et al., 2017b; Hawkins and Sutton, 2011; Shen et al., 2018), and our results indicate similar pattern for risk assessment.

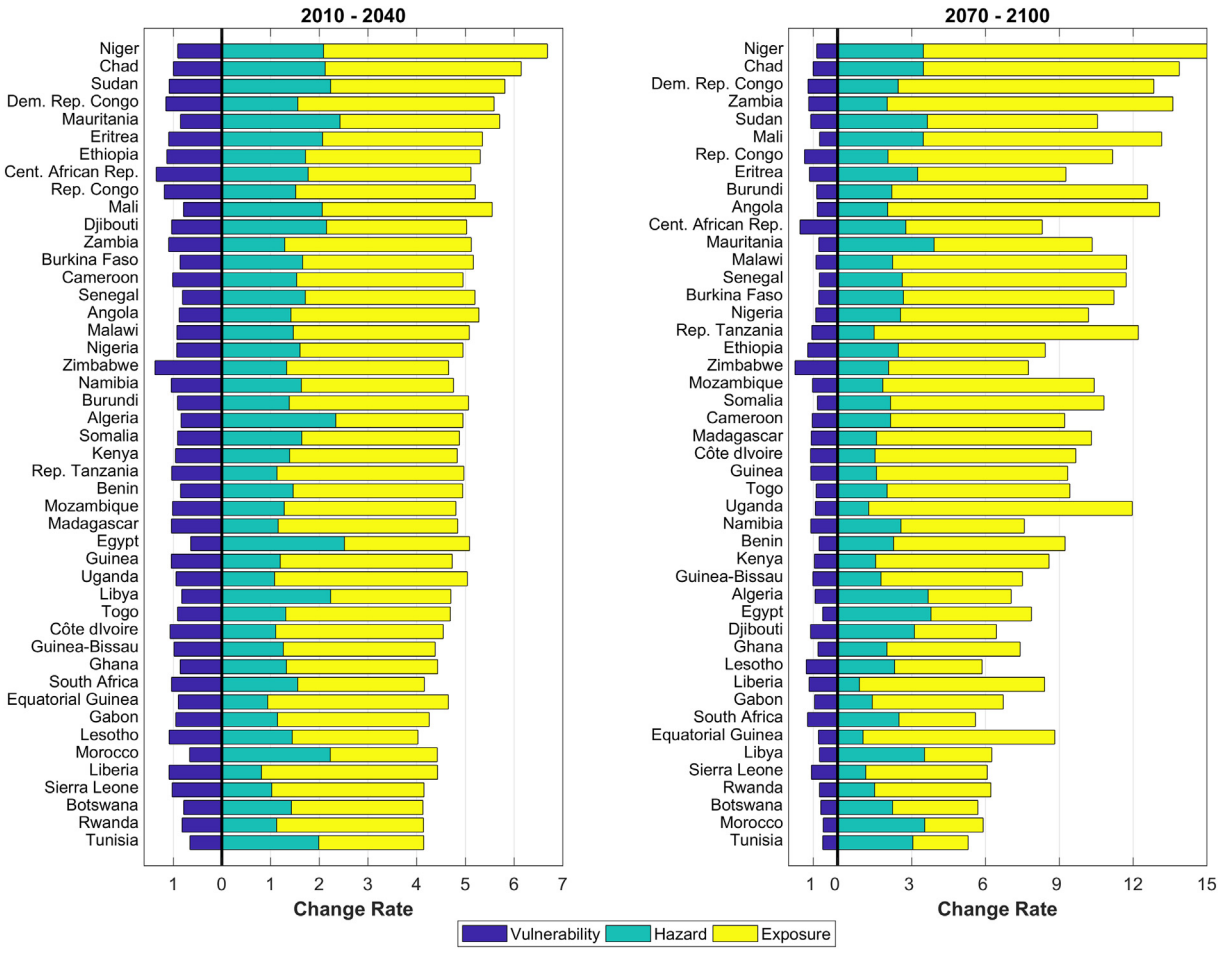

Fig. 10. Decomposition of drought risk components and their changes compared to the historical period. The figure shows the mean change rate among different scenarios, and the countries are arranged in descending order from the highest to lowest risk ratios.

This study presented a thorough assessment of the drought risk across the African continent using a top-down integrated drought risk modeling framework based on vulnerability, hazard, and exposure. The spatial patterns of drought risk in this study are consistent with earlier assessments (Kiguchi et al., 2015; Veldkamp et al., 2016). Brooks et al. (2005) classified the sub-Saharan African countries among the most vulnerable to climate hazards in the world. Carrao et al. (2016) assessed the current state of global drought risk and found the vulnerability and risks of the southern African countries lower than the central African nations. Furthermore, several other studies indicated similar spatial patterns for the impacts of climate change on drought hazard and water scarcity projections in Africa (Gosling and Arnell, 2016; Hanasaki et al., 2013; Liu et al., 2017; Schewe et al., 2014; Sheffield and Wood, 2008). The current study has built upon the previous analyses and it provides a multi-decadal drought risk assessment over the entire African continent using fine-resolution data and multi-model/scenario for each risk component.

Drought and water scarcity are among extreme challenges affecting the world, and climate change and population growth will exacerbate them (Hirabayashi et al., 2008; Mekonnen and Hoekstra, 2016). The issue is of higher concern for Africa, where the majority of countries have undeveloped economies faced with rapidly growing population, and they are unable to effectively use their resources (Neumayer, 2001). Results of this study identified increasing drought risk for the entire African continent, and the central African countries indicated the most severe aggravation. The results show that reducing net emissions to limit the global warming will substantially decrease drought risk, especially in distant future (Chen and Sun, 2017; Gudmundsson and Seneviratne, 2016). According to recent assessments, it is still feasible to limit global warming to <2 °C compared to the pre-industrialized era (Millar et al., 2017), albeit it is unlike to achieve it (Raftery et al., 2017). Therefore, the sooner climate change mitigation planning is worked upon, the higher is the chance to reduce the associated risks (Nangombe et al., 2018).

4. Summary and conclusion

This study investigated future drought risk in Africa considering components of vulnerability, hazard, and exposure. Drought vulnerability was quantified using a rigorous multi-dimensional framework consisting of 28 factors related to economy, energy and infrastructure, health, land use, society, and water resources, and three vulnerability scenarios were developed and employed for the analyses. An ensemble of 10 regional climate models (RCMs) was utilized for two emission scenarios of RCP4.5 and RCP8.5 to quantify drought hazard. Furthermore, three different population scenarios were employed to characterize the exposure to drought. Therefore, drought risk is quantified using a multi-model and multi-scenario approach, and the uncertainties associated with each source were characterized. The spatiotemporal trends and changing patterns of drought risk and its components were also investigated, and the main findings of the study are summarized as follows:

- Drought risk will increase in future for the entire African continent. The change rates are higher for central African countries.

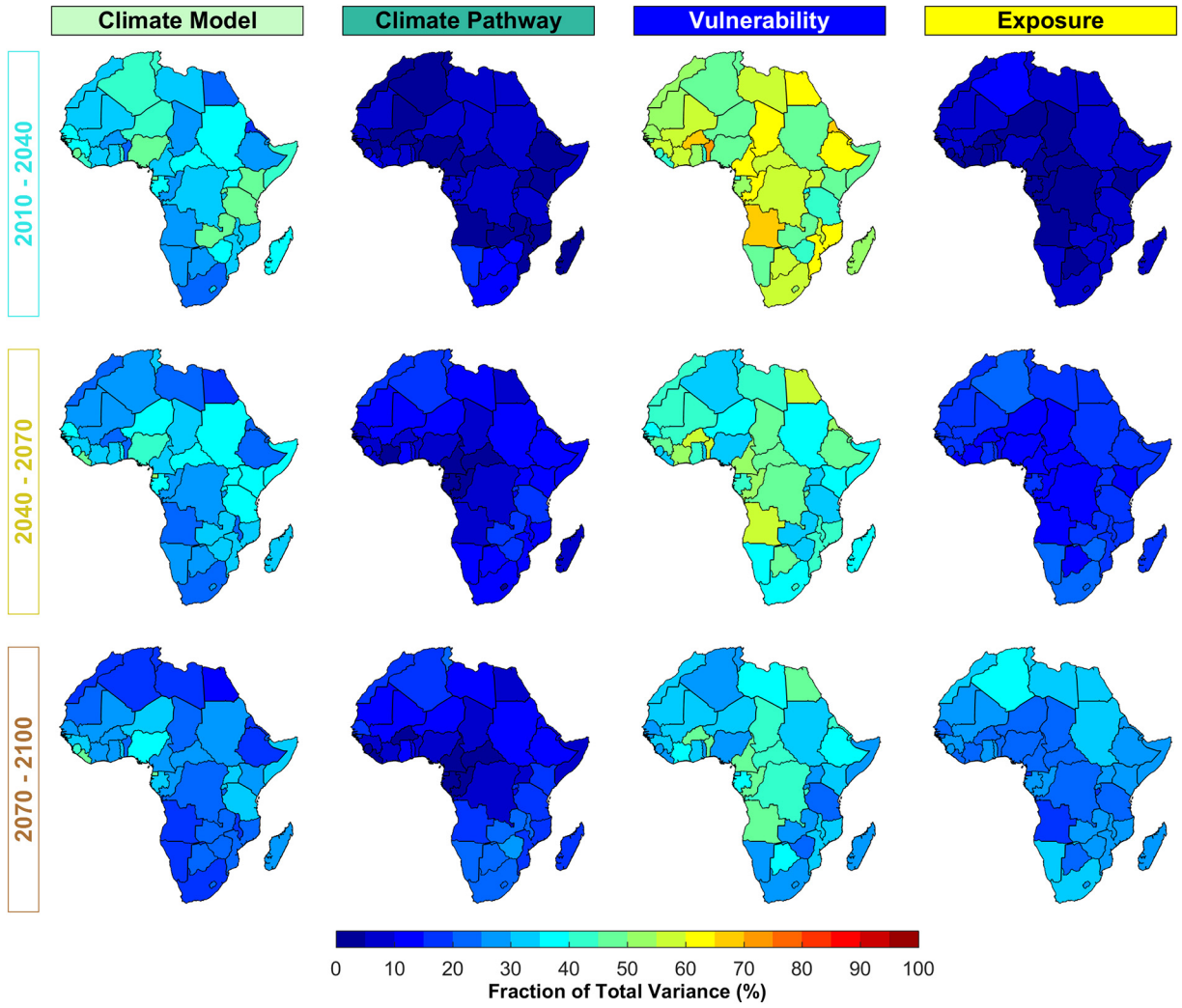

Fig. 11. Fraction of total variance of drought risk projections for each source of uncertainty in the future periods.

- Although risk ratios from different scenarios are similar in near future, vast differences are found between moderate and extreme scenarios (climate/vulnerability/population) in distant future.
- Niger and Chad indicate the highest drought risk ratios among other African countries, which is attributed to substantial population growth as well as increasing drought hazard due to climate change.

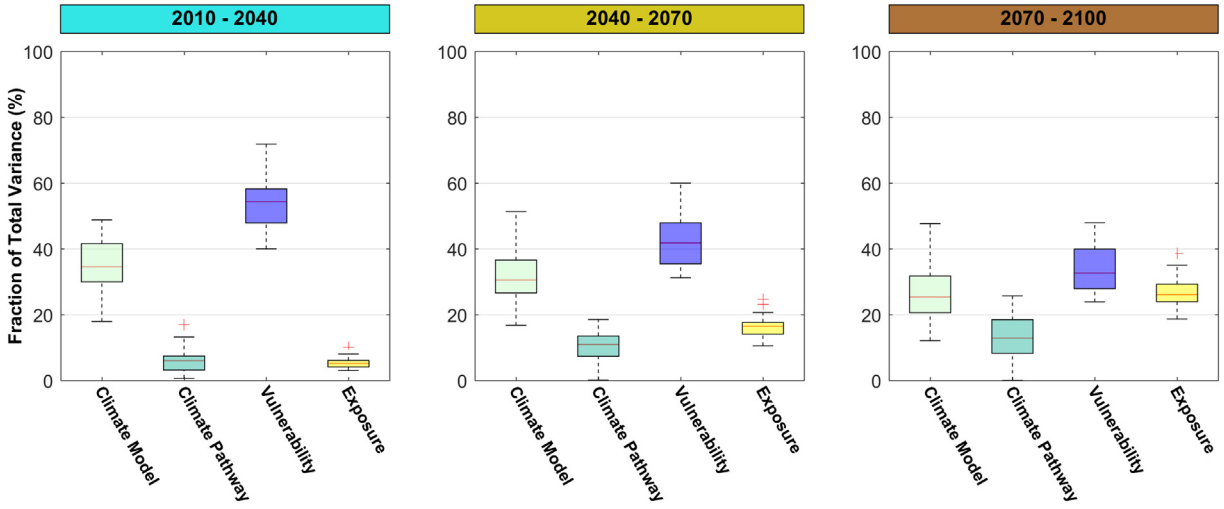

Fig. 12. The distribution of fraction of total variance among the 46 African countries for each source of uncertainty (indicated on x-axis) in three future periods. The red lines in the boxplots indicate the median value.

- Tunisia and Morocco indicate the lowest risk ratios (albeit significant increase in drought hazard), which is mainly attributed to advanced socioeconomic sectors that stabilize the population and decrease drought vulnerability.
- Population growth is a serious concern in Africa, as the majority of African countries are already dealing with limited natural and financial resources and impractical resource management practices, and it will further aggravate their social development.

Acknowledgement

We acknowledge the Coordinated Regional Climate Downscaling Experiment (CORDEX) for providing access to the regional climate model outputs and the United Nations for the population data that were used in this study.

Appendix A. Supplementary information

Supplementary data to this article can be found online at https://doi.org/10.1016/j.scitotenv.2019.01.278.

References

Ahmadalipour, A., Moradkhani, H., 2018a. Multi-dimensional assessment of drought vulnerability in Africa: 1960–2100. Sci. Total Environ. 644, 520–535. https://doi.org/10.1016/j.scitotenv.2018.07.023.

Ahmadalipour, A., Moradkhani, H., 2018b. Escalating heat-stress mortality risk due to global warming in the Middle East and North Africa (MENA). Environ. Int. 117, 215–225. https://doi.org/10.1016/j.envint.2018.05.014.

Ahmadalipour, A., Moradkhani, H., Demirel, M.C., 2017a. A comparative assessment of projected meteorological and hydrological droughts: elucidating the role of temperature. J. Hydrol. 553, 785–797. https://doi.org/10.1016/j.jhydrol.2017.08.047.

Ahmadalipour, A., Moradkhani, H., Svoboda, M., 2017b. Centennial drought outlook over the CONUS using NASA-NEX downscaled climate ensemble. Int. J. Climatol. 37, 2477–2491. https://doi.org/10.1002/joc.4859.

Antwi-Agyei, P., Fraser, E.D.G., Dougill, A.J., Stringer, L.C., Simelton, E., 2012. Mapping the vulnerability of crop production to drought in Ghana using rainfall, yield and socioeconomic data. Appl. Geogr. 32, 324–334.

Asadi Zarch, M.A., Sivakumar, B., Sharma, A., 2014. Droughts in a warming climate: a global assessment of standardized precipitation index (SPI) and reconnaissance drought index (RDI). J. Hydrol. https://doi.org/10.1016/j.jhydrol.2014.09.071.

Below, R., Grover-Kopec, E., Dilley, M., 2007. Documenting drought-related disasters: a global reassessment. J. Environ. Dev. 16, 328–344.

Birkmann, J., 2007. Risk and vulnerability indicators at different scales: applicability, usefulness and policy implications. Environ. Hazards 7, 20–31.

Birkmann, J., Cardona, O.D., Carreño, M.L., Barbat, A.H., Pelling, M., Schneiderbauer, S., Kienberger, S., Keiler, M., Alexander, D., Zeil, P., 2013. Framing vulnerability, risk and societal responses: the MOVE framework. Nat. Hazards 67, 193–211.

Blauhut, V., Gudmundsson, L., Stahl, K., 2015a. Towards pan-European drought risk maps: quantifying the link between drought indices and reported drought impacts. Environ. Res. Lett. 10, 14008.

Blauhut, V., Stahl, K., Stagge, J.H., Tallaksen, L.M., De Stefano, L., Vogt, J., 2015b. Estimating drought risk across Europe from reported drought impacts, hazard indicators and vulnerability factors. Hydrol. Earth Syst. Sci. Discuss. 12.

Brooks, N., Adger, W.N., Kelly, P.M., 2005. The determinants of vulnerability and adaptive capacity at the national level and the implications for adaptation. Glob. Environ. Chang. 15, 151–163.

Buhaug, H., Urdal, H., 2013. An urbanization bomb? Population growth and social disorder in cities. Glob. Environ. Chang. 23, 1–10.

Cai, X., Wallington, K., Shafiee-Jood, M., Marston, L., 2018. Understanding and managing the food-energy-water nexus–opportunities for water resources research. Adv. Water Resour. 111, 259–273.

Cardona, O.-D., van Aalst, M.K., Birkmann, J., Fordham, M., McGregor, G., Mechler, R., 2012. Determinants of risk: exposure and vulnerability. Managing the Risks of Extreme Events and Disasters to Advance Climate Change Adaptation. Cambridge University Press.

Carrao, H., Naumann, G., Barbosa, P., 2016. Mapping global patterns of drought risk: an empirical framework based on sub-national estimates of hazard, exposure and vulnerability. Glob. Environ. Chang. 39, 108–124.

Carrão, H., Naumann, G., Barbosa, P., 2017. Global projections of drought hazard in a warming climate: a prime for disaster risk management. Clim. Dyn. 1–19.

Checchi, F., Robinson, W.C., 2013. Mortality Among Populations of Southern and Central Somalia Affected by Severe Food Insecurity and Famine During 2010–2012. Food and Agriculture Organization of the United Nations.

Chen, H., Sun, J., 2017. Anthropogenic warming has caused hot droughts more frequently in China. J. Hydrol. 544, 306–318.

Chen, J., Brissette, F.P., Leconte, R., 2011. Uncertainty of downscaling method in quantifying the impact of climate change on hydrology. J. Hydrol. 401, 190–202.

Chen, G., Tian, H., Zhang, C., Liu, M., Ren, W., Zhu, W., Chappelka, A.H., Prior, S.A., Lockaby, G.B., 2012. Drought in the Southern United States over the 20th century: variability and its impacts on terrestrial ecosystem productivity and carbon storage. Clim. Chang. 114, 379–397. https://doi.org/10.1007/s10584-012-0410-z.

Cheng, L., Hoerling, M., AghaKouchak, A., Livneh, B., Quan, X.-W., Eischeid, J., 2015. How has human-induced climate change affected California drought risk? J. Clim. https://doi.org/10.1175/JCLI-D-15-0260.1 (151019113427001).

Cook, B.I., Ault, T.R., Smerdon, J.E., 2015. Unprecedented 21st century drought risk in the American Southwest and Central Plains. Sci. Adv. 1, 1–7. https://doi.org/10.1126/sciadv.1400082.

Dai, A., 2012. Increasing drought under global warming in observations and models. Nat. Clim. Chang. 3, 52–58.

Diasso, U., Abiodun, B.J., 2017. Drought modes in West Africa and how well CORDEX RCMs simulate them. Theor. Appl. Climatol. 128, 223–240.

Diffenbaugh, N.S., Swain, D.L., Touma, D., 2015. Anthropogenic warming has increased drought risk in California. Proc. Natl. Acad. Sci. 112, 201422385. https://doi.org/10.1073/pnas.1422385112.

Fekete, A., Hufschmidt, G., Kruse, S., 2014. Benefits and challenges of resilience and vulnerability for disaster risk management. Int. J. Disaster Risk Sci. 5, 3–20.

Gergel, D.R., Nijssen, B., Abatzoglou, J.T., Lettenmaier, D.P., Stumbaugh, M.R., 2017. Effects of climate change on snowpack and fire potential in the western USA. Clim. Chang. 141, 287–299.

Gerland, P., Raftery, A.E., Ševčíková, H., Li, N., Gu, D., Spoorenberg, T., Alkema, L., Fosdick, B.K., Chunn, J., Lalic, N., 2014. World population stabilization unlikely this century. Science (80-.) 346, 234–237.

Godfray, H.C.J., Beddington, J.R., Crute, I.R., Haddad, L., Lawrence, D., Muir, J.F., Pretty, J., Robinson, S., Thomas, S.M., Toulmin, C., 2010. Food security: the challenge of feeding 9 billion people. Science (80-.) 327, 812–818.

Gosling, S.N., Arnell, N.W., 2016. A global assessment of the impact of climate change on water scarcity. Clim. Chang. 134, 371–385.

Gudmundsson, L., Seneviratne, S.I., 2016. Anthropogenic climate change affects meteorological drought risk in Europe. Environ. Res. Lett. 11, 44005.

Han, L., Zhang, Q., Ma, P., Jia, J., Wang, J., 2016. The spatial distribution characteristics of a comprehensive drought risk index in southwestern China and underlying causes. Theor. Appl. Climatol. 124, 517–528.

Hanasaki, N., Fujimori, S., Yamamoto, T., Yoshikawa, S., Masaki, Y., Hijioka, Y., Kainuma, M., Kanamori, Y., Masui, T., Takahashi, K., 2013. A global water scarcity assessment under shared socio-economic pathways. Hydrol. Earth Syst. Sci. 17, 2393.

Hanjra, M.A., Qureshi, M.E., 2010. Global water crisis and future food security in an era of climate change. Food Policy 35, 365–377.

Hawkins, E., Sutton, R., 2011. The potential to narrow uncertainty in projections of regional precipitation change. Clim. Dyn. 37, 407–418. https://doi.org/10.1007/s00382-010-0810-6.

Hawkins, E., Smith, R.S., Gregory, J.M., Stainforth, D.A., 2015. Irreducible uncertainty in near-term climate projections. Clim. Dyn. https://doi.org/10.1007/s00382-015-2806-8.

Hirabayashi, Y., Kanae, S., Emori, S., Oki, T., Kimoto, M., 2008. Global projections of changing risks of floods and droughts in a changing climate. Hydrol. Sci. J. 53, 754–772.

Honda, Y., Kondo, M., McGregor, G., Kim, H., Guo, Y.-L., Hijioka, Y., Yoshikawa, M., Oka, K., Takano, S., Hales, S., 2014. Heat-related mortality risk model for climate change impact projection. Environ. Health Prev. Med. 19, 56–63.

IPCC, 2012. Managing the Risks of Extreme Events and Disasters to Advance Climate Change Adaptation: Special Report of the Intergovernmental Panel on Climate Change. Cambridge University Press.

Jones, C., Giorgi, F., Asrar, G., 2011. The Coordinated Regional Downscaling Experiment: CORDEX–an international downscaling link to CMIP5. CLIVAR Exch. 56, 34–40.

Jung, I.-W., Moradkhani, H., Chang, H., 2012. Uncertainty assessment of climate change impacts for hydrologically distinct river basins. J. Hydrol. 466, 73–87.

Kendall, M.G., 1948. Rank Correlation Methods.

Khan, Z.R., Midega, C.A.O., Pittchar, J.O., Murage, A.W., Birkett, M.A., Bruce, T.J.A., Pickett, J.A., 2014. Achieving food security for one million sub-Saharan African poor through push–pull innovation by 2020. Philos. Trans. R. Soc. Lond. Ser. B Biol. Sci. 369, 20120284.

Kiguchi, M., Shen, Y., Kanae, S., Oki, T., 2015. Re-evaluation of future water stress due to socio-economic and climate factors under a warming climate. Hydrol. Sci. J. 60, 14–29.

Kim, J., Waliser, D.E., Mattmann, C.A., Goodale, C.E., Hart, A.F., Zimdars, P.A., Crichton, D.J., Jones, C., Nikulin, G., Hewitson, B., 2014. Evaluation of the CORDEX-Africa multi-RCM hindcast: systematic model errors. Clim. Dyn. 42, 1189–1202.

Kim, H., Park, J., Yoo, J., Kim, T.-W., 2015. Assessment of drought hazard, vulnerability, and risk: a case study for administrative districts in South Korea. J. Hydro Environ. Res. 9, 28–35.

Li, X., He, B., Quan, X., Liao, Z., Bai, X., 2015. Use of the standardized precipitation evapotranspiration index (SPEI) to characterize the drying trend in southwest China from 1982–2012. Remote Sens. 7, 10917–10937. https://doi.org/10.3390/rs70810917.

Liu, J., Yang, H., Gosling, S.N., Kummu, M., Flörke, M., Pfister, S., Hanasaki, N., Wada, Y., Zhang, X., Zheng, C., 2017. Water scarcity assessments in the past, present and future. Earth's Future 5 (6), 545–559.

Lobell, D.B., Roberts, M.J., Schlenker, W., Braun, N., Little, B.B., Rejesus, R.M., Hammer, G.L., 2014. Greater sensitivity to drought accompanies maize yield increase in the US Midwest. Science (80-.) 344, 516–519.

Lyon, B., 2014. Seasonal drought in the Greater Horn of Africa and its recent increase during the March–May long rains. J. Clim. 27, 7953–7975.

Mekonnen, M.M., Hoekstra, A.Y., 2016. Four billion people facing severe water scarcity. Sci. Adv. 2, e1500323.

Millar, R.J., Fuglestvedt, J.S., Friedlingstein, P., Rogelj, J., Grubb, M.J., Matthews, H.D., Skeie, R.B., Forster, P.M., Frame, D.J., Allen, M.R., 2017. Emission budgets and pathways consistent with limiting warming to 1.5 °C. Nat. Geosci. 10, 741–747. https://doi.org/10.1038/ngeo3031.

Mishra, A., Vu, T., ValiyaVeettil, A., Entekhabi, D., 2017. Drought monitoring with soil moisture active passive (SMAP) measurements. J. Hydrol. 552, 620–632.

Mizukami, N., Clark, M.P., Gutmann, E.D., Mendoza, P.A., Newman, A.J., Nijssen, B., Livneh, B., Hay, L.E., Arnold, J.R., Brekke, L.D., 2016. Implications of the methodological choices for hydrologic portrayals of climate change over the contiguous United States: statistically downscaled forcing data and hydrologic models. J. Hydrometeorol. 17, 73–98.

Mukherjee, S., Mishra, A., Trenberth, K.E., 2018. Climate change and drought: a perspective on drought indices. Curr. Clim. Chang. Rep. 1–19.

Nangombe, S., Zhou, T., Zhang, W., Wu, B., Hu, S., Zou, L., Li, D., 2018. Record-breaking climate extremes in Africa under stabilized 1.5 °C and 2 °C global warming scenarios. Nat. Clim. Chang. 8, 375–380. https://doi.org/10.1038/s41558-018-0145-6.

Naumann, G., Barbosa, P., Garrote, L., Iglesias, A., Vogt, J., 2014a. Exploring drought vulnerability in Africa: an indicator based analysis to be used in early warning systems. Hydrol. Earth Syst. Sci. 18, 1591–1604.

Naumann, G., Dutra, E., Barbosa, P., Pappenberger, F., Wetterhall, F., Vogt, J.V., 2014b. Comparison of drought indicators derived from multiple data sets over Africa. Hydrol. Earth Syst. Sci. 18, 1625–1640.

Neumayer, E., 2001. The human development index and sustainability—a constructive proposal. Ecol. Econ. 39, 101–114.

Nicholson, S.E., 2014. A detailed look at the recent drought situation in the Greater Horn of Africa. J. Arid Environ. 103, 71–79. https://doi.org/10.1016/j.jaridenv.2013.12.003.

Nikiema, P.M., Sylla, M.B., Ogunjobi, K., Kebe, I., Gibba, P., Giorgi, F., 2017. Multi-model CMIP5 and CORDEX simulations of historical summer temperature and precipitation variabilities over West Africa. Int. J. Climatol. 37, 2438–2450.

Önol, B., Bozkurt, D., Turuncoglu, U.U., Sen, O.L., Dalfes, H.N., 2013. Evaluation of the twenty-first century RCM simulations driven by multiple GCMs over the Eastern Mediterranean–Black Sea region. Clim. Dyn. 42, 1949–1965. https://doi.org/10.1007/s00382-013-1966-7.

Peduzzi, P., Dao, Q.-H., Herold, C., Diaz, A.M., Mouton, F., Nordbeck, O., Rochette, D.S., Ton-That, T., Widmer, B., 2002. Global Risk and Vulnerability Index Trends per Year (GRAVITY) Phase II: Development, Analysis and Results.

Peduzzi, P., Dao, H., Herold, C., Mouton, F., 2009. Assessing global exposure and vulnerability towards natural hazards: the Disaster Risk Index. Nat. Hazards Earth Syst. Sci. 9, 1149–1159.

Peterson, T.C., Hoerling, M.P., Stott, P.A., Herring, S.C., 2013. Explaining extreme events of 2012 from a climate perspective. Bull. Am. Meteorol. Soc. 94, S1–S74.

Raftery, A.E., Zimmer, A., Frierson, D.M.W., Startz, R., Liu, P., 2017. Less than 2 °C warming by 2100 unlikely. Nat. Clim. Chang. 7, 637–641. https://doi.org/10.1038/nclimate3352.

Ring, C., Pollinger, F., Kaspar-Ott, I., Hertig, E., Jacobeit, J., Paeth, H., 2017. A comparison of metrics for assessing state-of-the-art climate models and implications for probabilistic projections of climate change. Clim. Dyn. 1–20.

Rossi, G., Cancelliere, A., 2013. Managing drought risk in water supply systems in Europe: a review. Int. J. Water Resour. Dev. 29, 272–289.

Schewe, J., Heinke, J., Gerten, D., Haddeland, I., Arnell, N.W., Clark, D.B., Dankers, R., Eisner, S., Fekete, B.M., Colón-González, F.J., 2014. Multimodel assessment of water scarcity under climate change. Proc. Natl. Acad. Sci. 111, 3245–3250.

Schilling, J., Freier, K.P., Hertig, E., Scheffran, J., 2012. Climate change, vulnerability and adaptation in North Africa with focus on Morocco. Agric. Ecosyst. Environ. 156, 12–26.

Schlosser, C.A., Strzepek, K., Gao, X., Fant, C., Blanc, É., Paltsev, S., Jacoby, H., Reilly, J., Gueneau, A., 2014. The future of global water stress: an integrated assessment. Earth's Future 2, 341–361.

Seto, K.C., Güneralp, B., Hutyra, L.R., 2012. Global forecasts of urban expansion to 2030 and direct impacts on biodiversity and carbon pools. Proc. Natl. Acad. Sci. 109, 16083–16088.

Sheffield, J., Wood, E., 2008. Projected changes in drought occurrence under future global warming from multi-model, multi-scenario, IPCC AR4 simulations. Clim. Dyn. 31, 79–105.

Shen, M., Chen, J., Zhuan, M., Chen, H., Xu, C.-Y., Xiong, L., 2018. Estimating uncertainty and its temporal variation related to global climate models in quantifying climate change impacts on hydrology. J. Hydrol. 556, 10–24.

Shiau, J.-T., Hsiao, Y.-Y., 2012. Water-deficit-based drought risk assessments in Taiwan. Nat. Hazards 64, 237–257.

Sivakumar, M.V.K., Stefanski, R., Bazza, M., Zelaya, S., Wilhite, D., Magalhaes, A.R., 2014. High level meeting on national drought policy: summary and major outcomes. Weather Clim. Extrem. 3, 126–132.

Smith, A.B., Katz, R.W., 2013. US billion-dollar weather and climate disasters: data sources, trends, accuracy and biases. Nat. Hazards 67, 387–410.

Smith, A.B., Matthews, J.L., 2015. Quantifying uncertainty and variable sensitivity within the US billion-dollar weather and climate disaster cost estimates. Nat. Hazards 77, 1829–1851.

Stagge, J.H., Kohn, I., Tallaksen, L.M., Stahl, K., 2015. Modeling drought impact occurrence based on meteorological drought indices in Europe. J. Hydrol. 530, 37–50. https://doi.org/10.1016/j.jhydrol.2015.09.039.

Svoboda, M.D., Fuchs, B.A., Poulsen, C.C., Nothwehr, J.R., 2015. The drought risk atlas: enhancing decision support for drought risk management in the United States. J. Hydrol. 526, 274–286.

Tánago, I.G., Urquijo, J., Blauhut, V., Villarroya, F., De Stefano, L., 2016. Learning from experience: a systematic review of assessments of vulnerability to drought. Nat. Hazards 80, 951–973.

Touma, D., Ashfaq, M., Nayak, M.a., Kao, S.-C., Diffenbaugh, N.S., 2015. A multi-model and multi-index evaluation of drought characteristics in the 21st century. J. Hydrol. 526, 196–207. https://doi.org/10.1016/j.jhydrol.2014.12.011.

UNISDR, 2015. Sendai Framework for Disaster Risk Reduction 2015–2030 (Geneva, Switzerland, WWW Document).

United Nations, Department of Economic and Social Affairs, P.D, 2015. World Population Prospects: The 2015 Revision, DVD Edition.

Veldkamp, T.I.E., Wada, Y., Aerts, J., Ward, P.J., 2016. Towards a global water scarcity risk assessment framework: incorporation of probability distributions and hydro-climatic variability. Environ. Res. Lett. 11, 24006.

Vicente-Serrano, S.M., Beguería, S., López-Moreno, J.I., 2010. A multiscalar drought index sensitive to global warming: the standardized precipitation evapotranspiration index. J. Clim. 23, 1696–1718. https://doi.org/10.1175/2009JCLI2909.1.

Vicente-Serrano, S.M., Beguería, S., Gimeno, L., Eklundh, L., Giuliani, G., Weston, D., El Kenawy, A., López-Moreno, J.I., Nieto, R., Ayenew, T., 2012. Challenges for drought mitigation in Africa: the potential use of geospatial data and drought information systems. Appl. Geogr. 34, 471–486.

Vörösmarty, C.J., Green, P., Salisbury, J., Lammers, R.B., 2000. Global water resources: vulnerability from climate change and population growth. Science (80-.) 289, 284–288.

Wilhite, D.A., Sivakumar, M.V.K., Pulwarty, R., 2014. Managing drought risk in a changing climate: the role of national drought policy. Weather Clim. Extrem. 3, 4–13.

Xie, W., Xiong, W., Pan, J., Ali, T., Cui, Q., Guan, D., Meng, J., Mueller, N.D., Lin, E., Davis, S.J., 2018. Decreases in global beer supply due to extreme drought and heat. Nat. Plants 4, 964.

Zhao, T., Dai, A., 2017. Uncertainties in historical changes and future projections of drought. Part II: model-simulated historical and future drought changes. Clim. Chang. 144, 535–548.

Zscheischler, J., Westra, S., Hurk, B.J.J.M., Seneviratne, S.I., Ward, P.J., Pitman, A., AghaKouchak, A., Bresch, D.N., Leonard, M., Wahl, T., 2018. Future climate risk from compound events. Nat. Clim. Chang. 1.